

# FEASIBILITY OF IN-LINE STRESS MEASUREMENT BY CONTINUOUS BARKHAUSEN METHOD

FINAL REPORT  
*with*  
GUIDELINES FOR COMMERCIAL DEVELOPMENT  
Contract No. DTRS5602T0003  
SwRI® Project 14.06172

*Prepared for*

United States Department of Transportation  
Research and Special Programs Administration (RSPA)  
Office of Contracts and Procurement, DMA-30  
400 7th Street, S.W., Room 7104  
Washington, D.C. 20590

*Prepared by*

Sensor Systems and NDE Technology Department  
Applied Physics Division  
Southwest Research Institute®

"DISTRIBUTION STATEMENT. Distribution authorized to U.S. Government agencies only to protect information protected by a contractor's "limited rights" statement, or received with the understanding that it will not be routinely transmitted outside the U.S. Government. Other requests for this document are to be referred to the Project Manager."

August 2004



SOUTHWEST RESEARCH INSTITUTE  
SAN ANTONIO  
DETROIT  
HOUSTON  
WASHINGTON, DC

# FEASIBILITY OF IN-LINE STRESS MEASUREMENT BY CONTINUOUS BARKHAUSEN METHOD

FINAL REPORT  
*with*  
GUIDELINES FOR COMMERCIAL DEVELOPMENT  
Contract No. DTRS5602T0003  
SwRI Project 14.06172

*Prepared for*

United States Department of Transportation  
Research and Special Programs Administration (RSPA)  
Office of Contracts and Procurement, DMA-30  
400 7th Street, S.W., Room 7104  
Washington, D.C. 20590

*Prepared by*

Sensor Systems and NDE Technology Department  
Applied Physics Division  
Southwest Research Institute

August 2004

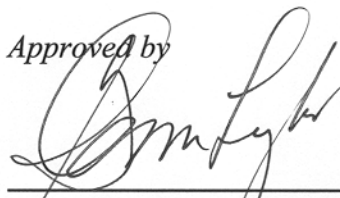
*Written by*



---

Alfred E. Crouch, P.E.  
Staff Engineer

*Approved by*



---

Glenn M. Light, Ph.D.  
Director

## **ACKNOWLEDGMENTS**

Southwest Research Institute and the author of this report gratefully acknowledge the financial and management support provided by the U.S. Department of Transportation and H. Rosen GmbH. Specific mention should be made of Messrs. James Merritt and Wade Van Nguyen of the DOT's Research and Special Programs Administration and Bryce Brown and Thomas Beuker of H. Rosen GmbH.

# TABLE OF CONTENTS

|  | <u>Page</u> |
|--|-------------|
| 1. INTRODUCTION .....                                | 1           |
| 2. BARKHAUSEN METHOD .....                           | 2           |
| 2.1 Standard NDE Applications.....                   | 2           |
| 2.2 Continuous Barkhausen .....                      | 4           |
| 2.3 SwRI Early Work.....                             | 4           |
| 2.4 Application to MFL Pigs .....                    | 5           |
| 2.5 MFL Pig Design.....                              | 5           |
| 2.5.1 Determine Optimum Sensor Location.....         | 7           |
| 2.5.2 Determine Optimum Sensor Design.....           | 7           |
| 2.5.3 Coil Orientation .....                         | 7           |
| 2.5.4 Liftoff Sensitivity .....                      | 10          |
| 2.6 Magnetizer Strength Test.....                    | 10          |
| 2.7 Pipe Speed Test.....                             | 10          |
| 2.8 Pull Rig Testing .....                           | 13          |
| 2.9 Rosen Pull Tests.....                            | 17          |
| 2.9.1 Test Line.....                                 | 17          |
| 2.9.2 Defects.....                                   | 19          |
| 2.9.3 Procedure.....                                 | 19          |
| 2.9.4 Findings.....                                  | 20          |
| 2.9.5 Conclusions from Rosen Pull Test .....         | 24          |
| 3. CONCLUSIONS AND RECOMMENDATIONS .....             | 25          |
| 3.1 CBN Measuring Ability.....                       | 25          |
| 3.2 Practical Considerations for Use on MFL Pig..... | 25          |
| 4. FINANCIAL STATUS REPORT.....                      | 26          |
| 5. BIBLIOGRAPHY .....                                | 27          |
| APPENDIX A — GUIDELINES FOR COMMERCIAL DEVELOPMENT   |             |

## LIST OF FIGURES

| <u>Figure</u> |   | <u>Page</u> |
|---------------|---|-------------|
| 1             | Block diagram of conventional Barkhausen system.....  | 3           |
| 2             | Basic Barkhausen response with sawtooth excitation .....  | 3           |
| 3             | SwRI research setup for evaluation of continuous Barkhausen concept .....   | 4           |
| 4             | Cross section of magnetizer of typical MFL pig .....  | 6           |
| 5             | Lab specimen showing sensor at trailing pole edge.....  | 8           |
| 6             | 19-mm × 6-mm × 6-mm, 500-turn coil.....   | 8           |
| 7             | Simulated defect.....   | 9           |
| 8             | Test setup .....  | 9           |
| 9             | Effect of probe angle on Barkhausen signal .....  | 11          |
| 10            | Average detected signal .....   | 11          |
| 11            | Barkhausen noise vs. magnetizer current.....  | 12          |
| 12            | Effect of surface speed.....  | 12          |
| 13            | 16-inch test specimen after defects were installed.....   | 14          |
| 14            | Internal peened defect .....  | 14          |
| 15            | External quenched defect.....   | 15          |
| 16            | Nondestructive surface stress measurements made to characterize<br>internal and external defects prior to pull testing..... | 15          |
| 17            | Amplifier/filter interface filter boards .....  | 16          |
| 18            | Acetylene torch and water hose are used to make a quench zone<br>on the test line .....                                     | 16          |
| 19            | Test line as seen from launch end.....  | 17          |
| 20            | Sensor mounted rigidly to magnetizer .....  | 19          |
| 21            | Amplifier box containing bandpass amplifiers and detector .....   | 19          |
| 22            | Instrumentation complement for pull testing.....  | 20          |
| 23            | External sensors at external quench defect .....  | 21          |
| 24            | External sensors at external grind mark.....  | 21          |

## LIST OF FIGURES

| <b><u>Figure</u></b> |  | <b><u>Page</u></b> |
|----------------------|--|--------------------|
| 25                   | Differential signal from sensors at external quench defect.....      | 22                 |
| 26                   | Differential signal from external grind marks .....                  | 22                 |
| 27                   | Heavy wall specimen .....  | 23                 |
| 28                   | Light wall specimen.....   | 23                 |
| 29                   | Differential sensor data smoothed with a running average filter..... | 23                 |
| 30                   | Smoothed differential data from subsequent run .....                 | 24                 |

# 1. INTRODUCTION

Southwest Research Institute (SwRI) pioneered the use of the Barkhausen effect for stress measurement in the 1960s, and the method is still in use today. Dr. David Atherton<sup>1</sup> at Queen's University has successfully used the technique to determine stress magnitude and direction. Atherton's technique, as did the earliest SwRI work, requires an alternating magnetic excitation field and an inductive sensor that responds to the Barkhausen magnetic transitions.

It has been shown clearly in Atherton's work, as well as that of other researchers,<sup>2</sup> that locally stressed areas in pipelines produce Barkhausen response. While the Barkhausen method has been widely applied for stress measurement, no practical deployment of Barkhausen sensors has been accomplished inside an operating pipeline. The advantages offered by coupling Barkhausen sensors to the magnetic circuit of an existing MFL smart pig may make it feasible to make Barkhausen measurements inside a pipe, thereby detecting local stress anomalies, which could include mechanical damage, hard spots, and potentially even stress corrosion cracking.

In contrast to the traditional Barkhausen implementation, the continuous Barkhausen noise concept does not require an alternating excitation field, relying instead on the field transition already present as an MFL pig moves through the pipeline. All magnetic flux leakage (MFL) pigs in use today, whether using permanent magnets or electromagnets, are creating Barkhausen noise as they move through the pipeline. The only requirements for using those signals are to provide suitable sensors and amplifiers and to develop a data interpretation procedure.

This report discusses the Barkhausen method and the implementation of continuous Barkhausen sensing on an MFL smart pig. Supporting experiments in the laboratory and pull testing are described, and results from simulated pipeline defects are presented. Guidelines for commercial development are included in Appendix A.

---

<sup>1</sup> Dr. Atherton's Applied Magnetism Group at Queen's University has published widely on the Barkhausen measurement of stress. A collection of those publications is in the bibliography at the end of this report.

<sup>2</sup> B. Augustyniak, M. Chmielewski, L. Piotrowski, T. Skibinski, D. Mezyk. "Residual Stress Evaluation in Oil Pipeline." *Proceedings of the 4th International Conference on Barkhausen Noise and Micromagnetic Testing*, Brescia, 03-04.07.2003. Editors: G. Conzella, E. Sardini, A. S. Wojtas, and T. Sourtini-Suominen. Wydawca: Stresstech Oy, Tikkutehtaantie, Finland; 2003 s. 187-196.

## 2. BARKHAUSEN METHOD

Dr. Heinrich Barkhausen was the German physicist who discovered the Barkhausen effect, a principle concerning changes in the magnetic state of ferromagnetic metal. In 1919, Barkhausen's work in acoustics and magnetism led to the discovery of the Barkhausen effect, which provided evidence that magnetization affects whole domains of a ferromagnetic material, rather than individual atoms alone. The Barkhausen effect concerns the sudden changes in the size and orientation of ferromagnetic domains that occur during magnetization or demagnetization. Barkhausen discovered that a slow increase of a magnetic field applied to a piece of ferromagnetic material causes it to become magnetized in minute increments.

The sudden jumps in magnetization may be detected by a coil of wire wound on the ferromagnetic material. The transitions in the magnetic field of the material produce pulses of current in the coil. These jumps are interpreted as discrete changes in the size or rotation of ferromagnetic domains.

Barkhausen noise may be used to analyze a material's physical characteristics. This type of analysis is also referred as the magnetoelastic or the micromagnetic method. Many common surface treatments such as grinding, shot peening, and induction hardening involve modification of both stress and microstructure and produce a response from the Barkhausen method. Processes such as fatigue similarly involve changes in stress and microstructure and can also be monitored with Barkhausen noise. Further information on Dr. Barkhausen's work can be found at [http://www.geocities.com/neveyaakov/electro\\_science/Barkhausen.html](http://www.geocities.com/neveyaakov/electro_science/Barkhausen.html).

### 2.1 Standard NDE Applications

In the standard use of the Barkhausen technique, the domain arrangement is altered by a controlled time-rate-of-change of an externally applied magnetic field, and the Barkhausen jumps are detected as voltage pulses induced into a small induction sensing coil located at the surface of the specimen, an arrangement illustrated in Figure 1. In the usual application, the magnetic yoke, specimen, and sensing probe are stationary.

Figure 2 illustrates the generation of Barkhausen noise in response to a sawtooth excitation of an electromagnet. Note that the burst of RF energy (the Barkhausen noise) occurs shortly past the zero crossing of the excitation waveform in both the positive going and negative going current directions. The greatest amplitude of Barkhausen is seen to be before the knee of the B-H curve of the material, with amplitude dropping off past the knee. Note that the RF waveforms are not identical. There is a large random component to the details of the energy waveform, but the total energy is very repeatable.

Development of the Barkhausen noise stress measurement technique at SwRI resulted in a number of important exploratory applications, including residual stress measurement in helicopter rotor blade spars and auto-frettagged gun tubes. Equipment sensitivity was increased enough to enable useful measurements to be made on rolling element-bearing components in which the Barkhausen effect is normally difficult to detect. Notwithstanding these advances, the Barkhausen technique remained an essentially stationary technique, requiring time for the excitation field to cycle and for the sensor to collect the noise signals.

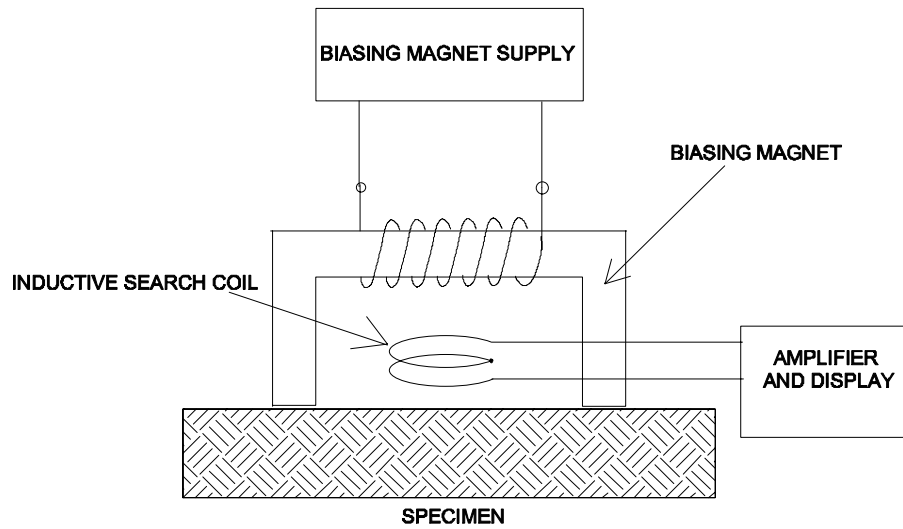


Figure 1. Block diagram of conventional Barkhausen system

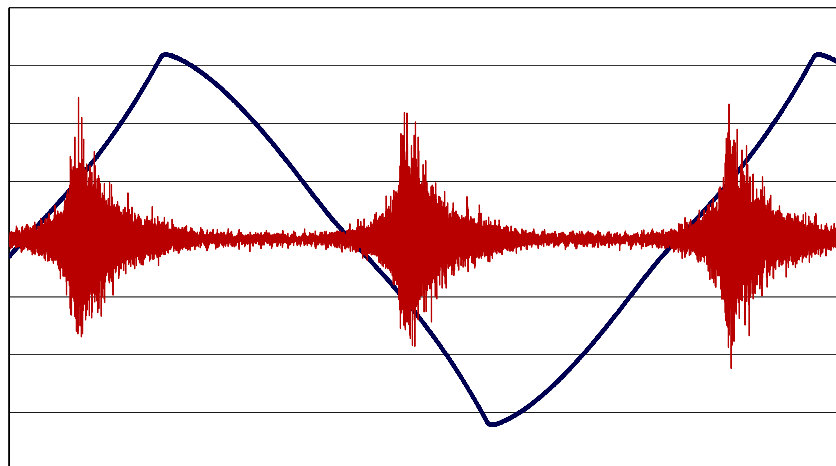


Figure 2. Basic Barkhausen response with sawtooth excitation

## 2.2 Continuous Barkhausen

The possibility of continuously obtaining Barkhausen noise is based on the reasonable hypothesis that, as an alternative to the standard method of cycling the magnetic field applied to the specimen, the specimen magnetization could also be changed by physically moving, in the vicinity of the specimen, a magnet producing a steady-state field. To demonstrate the feasibility of such an approach to obtaining continuous Barkhausen signals, SwRI funded an internal research program

## 2.3 SwRI Early Work

SwRI conducted experiments to validate the premise that Barkhausen noise was generated in the transition zone next to a magnetic exciter. The results were positive and gave confidence that similar signals would be found next to the magnetizer poles in an MFL pig. The apparatus used at SwRI to investigate the CBN concept is shown in Figure 3.

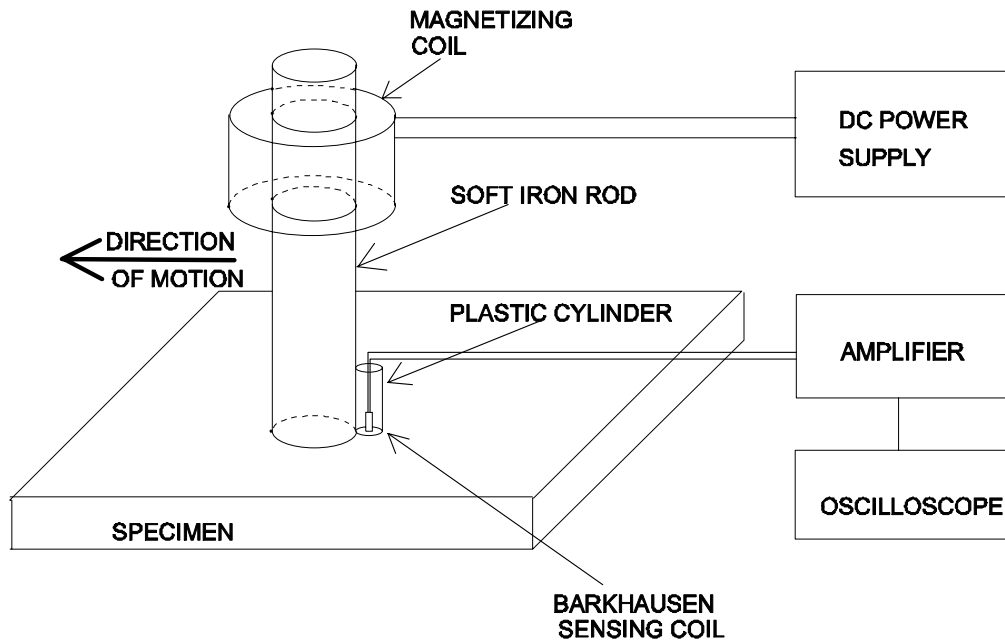


Figure 3. SwRI research setup for evaluation of continuous Barkhausen concept

The primary field was established by a solenoid coil energized with direct current. The field developed in the soft iron rod impinged on the test specimen and magnetized the zone adjacent the rod end. A small plastic cylinder was attached to the iron rod, placing the Barkhausen sensing coil directly above the zone of magnetic domain reorientation. As the iron rod assembly was moved over the specimen, the specimen surface under the sensing coil was continually subjected to a changing magnetic state; thus, the sensor was continually detecting Barkhausen signals. Since those Barkhausen signals vary with specimen stress, there should be a noticeable change in Barkhausen output when the probe is moved from an unstressed area to a stressed one. For example, in one SwRI experiment, a 2:1 change in signal level was noted when moving from a shot-peened area to an unpeened one.

## **2.4 Application to MFL Pigs**

One difficulty identified in the SwRI tests was being able to scan in the presence of the strong attractive force between the iron core and the specimen. This would not be a problem for the pipeline pig case because the pig cups and brushes are in contact with the pipe surface and keep the pig centered as it moves through the pipe.

## **2.5 MFL Pig Design**

By far, the most common technology for in-line detection of pipeline corrosion is the magnetic flux leakage (MFL) method, so named because the concept is illustrated by diagrams of pipe walls with reduced cross section at which induced magnetic fields divert from their primary metal path and “leak” out of the pipe wall into the surrounding air, where they may be detected by suitable magnetic field sensors. The induced magnetic field is provided by permanent magnets or electromagnets coupled to the pipe wall by steel brushes or very short air gaps. Sensors, which can be wire coils, Hall effect probes, or other solid-state detectors are generally positioned between the poles of the magnetizer, where the magnetic field in the pipe wall is strong and well controlled.

Defect signals, which may be in the microvolt or low millivolt range, are amplified and recorded. In some cases, bandwidths are reduced to improve the signal-to-noise ratio. After the inspection vehicle has been removed from the pipe and the data recovered, the MFL data are analyzed to determine the severity of any detected defects.

The operating environment for ILI systems is not a friendly one. The primary contributors to the challenging environment are:

- (1) Surrounding media that may include crude oil, natural gas, carbon dioxide, or refined petroleum products. There may also be corrosive components in any of these materials.
- (2) High operating pressures that are capable of forcing the pumped product into sealed or encapsulated components and potentially damaging circuits or sensors.
- (3) Significant shocks and vibration as the pig moves through the pipeline. The pig is necessarily in contact with the pipe inner surface, and thus contacts girth welds every 40 feet, side openings (branch connections), and other pipeline appurtenances.

- (4) Paraffin deposits and debris can interfere with sensor contact with the pipe wall and can impact the movement of linkages or other mechanical parts of the pig.
- (5) Potentially high temperatures near compressor discharge and low flash temperatures as gas pipeline receiver traps are bled off to remove the pig.

Figure 4 shows a cross section of a typical MFL pig magnetizer. The magnetic field for MFL inspection is established in the pipe wall between brushes. The pipe wall regions ahead of the pig and behind it are at a magnetic state of lower intensity than the zone between the brushes, and the greatest gradient in the magnetic field is found in the transition zones shown in the figure. In those zones, the field is changing direction and magnitude, so the magnetic domain movement produces Barkhausen noise.

Because of the high field gradient, the optimum location for Barkhausen sensors should be near the leading or trailing edges of the magnetizer.

Barkhausen sensors are typically inductive (wire coils) with or without cores. Coils have advantages, particularly in the region near the magnet poles, because they do not experience saturation from strong bias fields. The coil is inherently “a-c coupled” and can detect small field variations in the presence of a strong d-c field component, whereas the d-c field may saturate a solid-state sensor such as a Hall element, rendering it insensitive to small field changes.

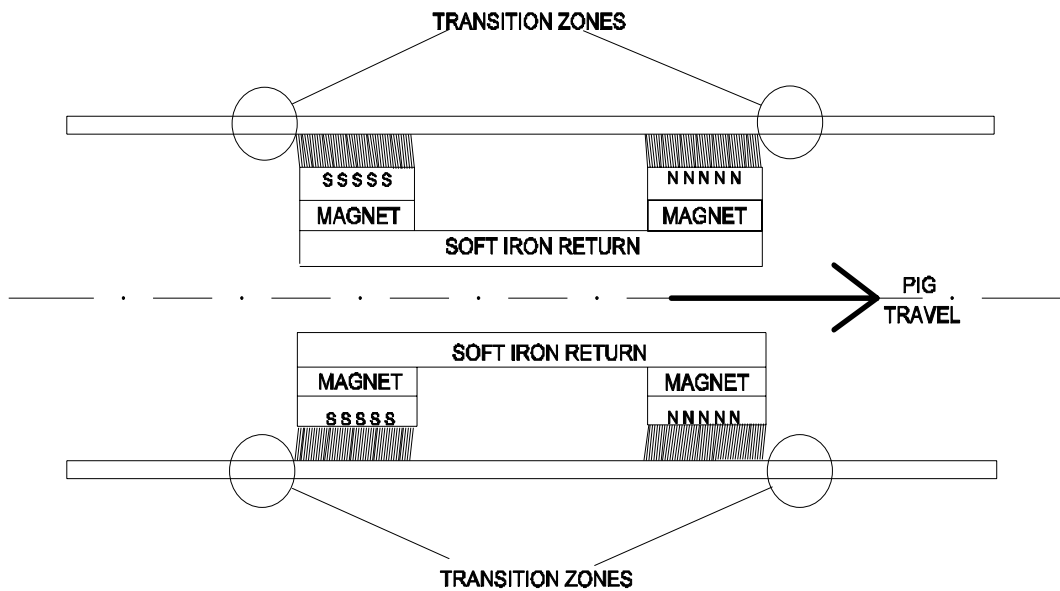


Figure 4. Cross section of magnetizer of typical MFL pig

### ***2.5.1 Determine Optimum Sensor Location***

Sensor location is critical because Barkhausen noise is generated by changes in the magnetization of the pipe wall, but predominantly at one region of the magnetization curve. In this investigation, finite element modeling was used to evaluate the potential locations on an MFL pig in a pipe section where the Barkhausen noise with the optimum signal-to-noise ratio may be detectable. Our commercial partner in the project, H. Rosen GmbH, provided us with extensive magnetic maps of the magnetic flux leakage in the sensor area of one of their inspection pigs. These data were used in the modeling effort. The finite element modeling revealed that the maximum amount of Barkhausen signal would be found at the edge of the trailing magnetizing pole, as shown in Figure 5. This was confirmed experimentally.

### ***2.5.2 Determine Optimum Sensor Design***

A design was developed for a sensor coil. The design and orientation of the coil were validated experimentally in laboratory tests using a rotating pipe section containing a simulated defect. Several coil sizes were evaluated, and the best results were obtained from a 19-mm × 6-mm × 6-mm, 500-turn coil. The coil is shown in Figure 6. Figure 7 shows the simulated defect, which is the peened portion of the pipe section. Impacting the pipe surface with a pneumatic needle scaler imparted stress that was detectable from Barkhausen noise signals. The test setup is shown in Figure 8.

Coil orientation and liftoff were investigated as part of this task. The sensitivity of the coil as a function of coil orientation with respect to the magnetic field was also experimentally evaluated. The sensitivity to coil liftoff was investigated by moving the coil away from the pipe surface and monitoring the signal.

Frequency discrimination was also investigated in an attempt to improve the signal-to-noise ratio. The best results were obtained using a 40- to 80-kHz bandpass filter.

### ***2.5.3 Coil Orientation***

A general understanding of Barkhausen technology suggests that the maximum probe sensitivity should be obtained when the probe sensitive axis is parallel to the applied magnetic field. We were interested in knowing how rapidly this maximum signal would fall off when the probe axis was made nonparallel to the field. Using AC excitation and the small hand-held probe, we collected data as the probe angle was changed from zero to 90 degrees from the ideal position.

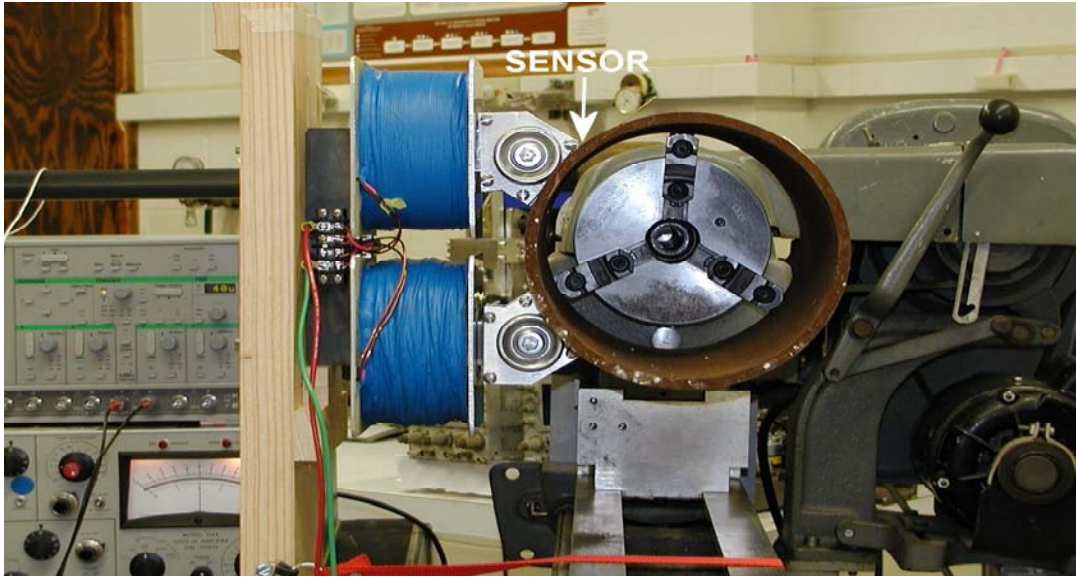


Figure 5. Lab specimen showing sensor at trailing pole edge

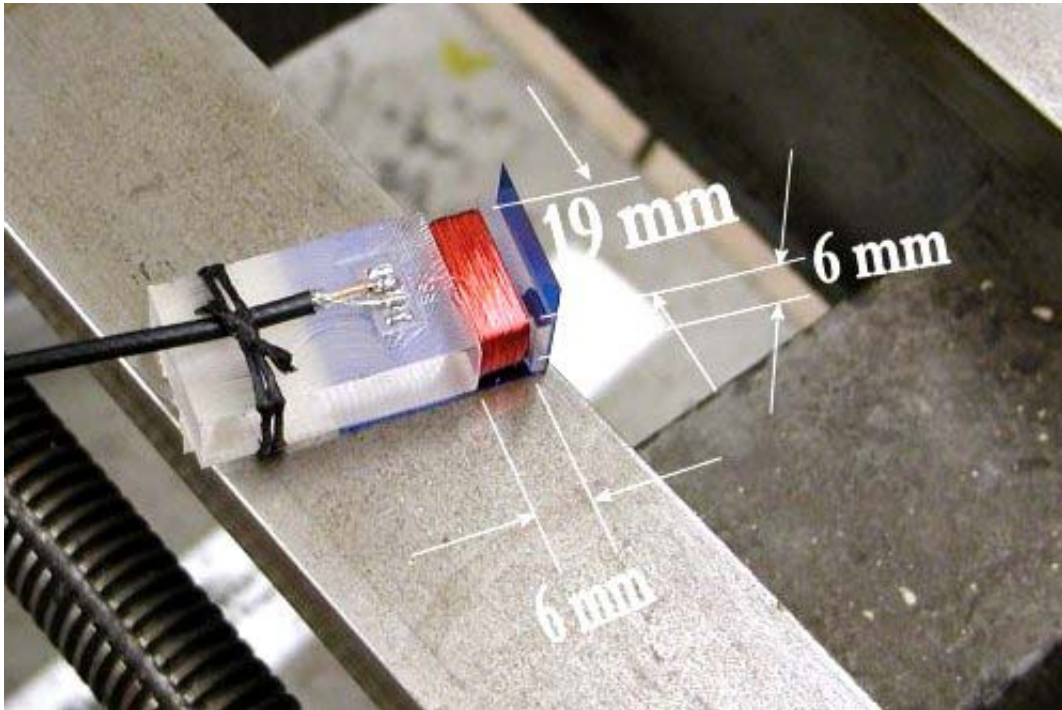


Figure 6. 19-mm  $\times$  6-mm  $\times$  6-mm, 500-turn coil



Figure 7. Simulated defect



Figure 8. Test setup

Figure 9 shows the angle response. The reduction in signal sensitivity at the orthogonal position is approximately 38 percent compared to the in-line position.

#### **2.5.4 *Liftoff Sensitivity***

To determine the liftoff sensitivity, an AC system was used to collect Barkhausen data using a small hand-held coil. Figure 10 shows the rapid drop-off of signal.

Note that for this coil, any liftoff greater than about 1 mm would be too great. The larger coil we used for later tests would not have this steep response and could tolerate liftoff up to several millimeters.

### **2.6 Magnetizer Strength Test**

We expected the Barkhausen signal to increase with increasing magnetizer power, but did not know what that relationship would look like, so we used the rotating specimen and the electromagnet to collect Barkhausen data for magnetizer currents from zero to the maximum permissible by our power supply. The data are graphed in Figure 11.

Note that the response does not show indication of saturation on the top, so we may conclude we have not passed the knee of the curve for the pipe wall.

### **2.7 Pipe Speed Test**

To determine the effect of pig speed, we used our lab fixture to run various pipe rotation speeds and collect data from the defect. The results were calculated in terms of pipe surface speeds (see Figure 12).

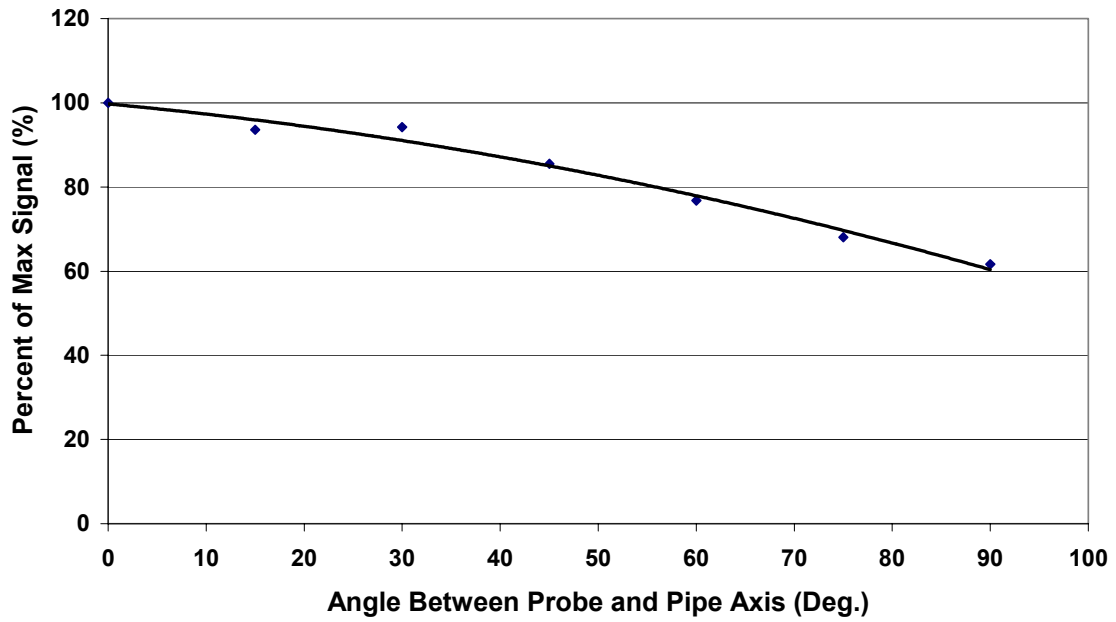


Figure 9. Effect of probe angle on Barkhausen signal

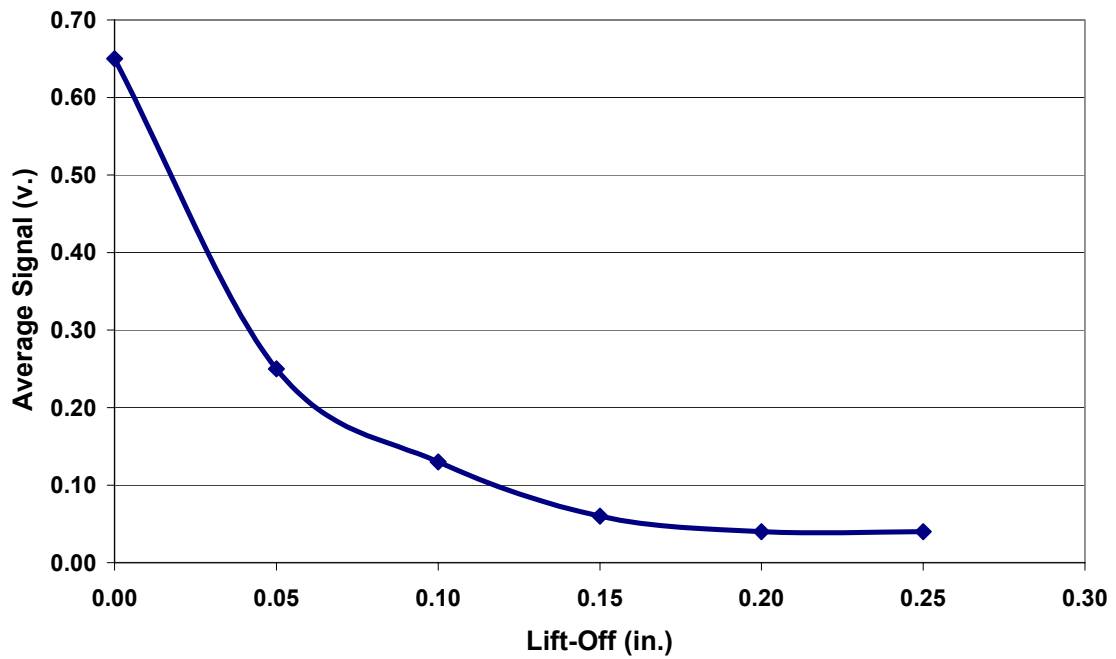


Figure 10. Average detected signal

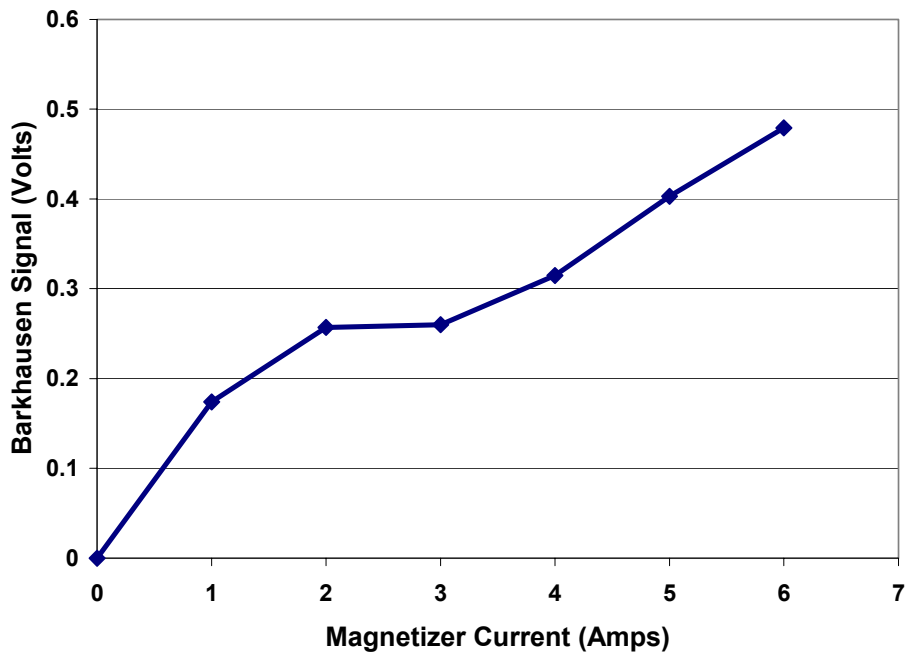


Figure 11. Barkhausen noise vs. magnetizer current

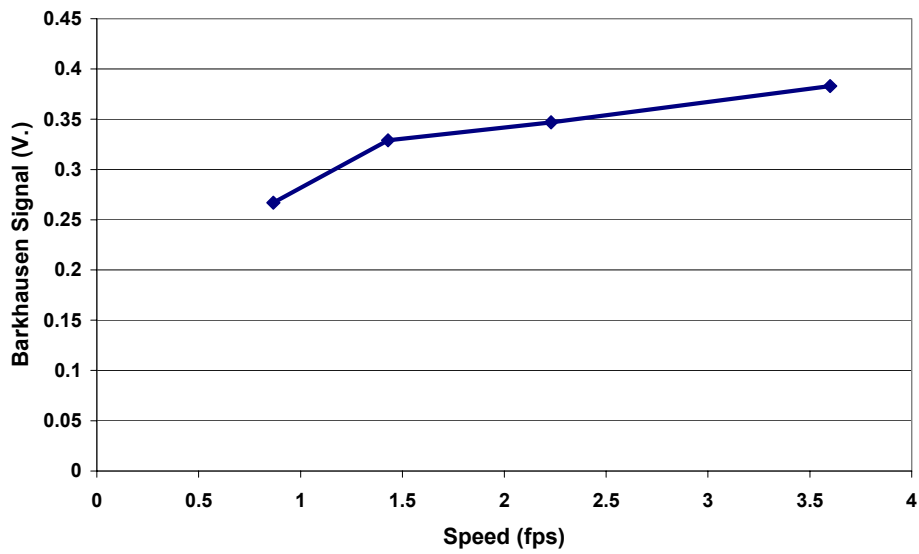


Figure 12. Effect of surface speed

## 2.8 Pull Rig Testing

Following the successful laboratory testing, the next step was to add the CBN sensors to an MFL magnetizer and demonstrate CBN in pull testing through actual line pipe specimens. Pull testing was arranged with cooperation of the cofunding partner, H. Rosen Inspection, of Houston, Texas. They made their pull rig and a 16-inch MFL magnetizer available for the testing.

Two joints of 16-inch pipe were purchased for test specimens. Wall thicknesses were 0.188 and 0.375 inch (9.5 mm).

Each SwRI test joint had 11 artifacts installed that could be detectable either by MFL, Barkhausen, or both. The primary Barkhausen defects were 2-inch (50-mm) (axial) × 10-inch (200-mm) (circumferential) inside-surface stressed areas created by either peening or quenching. In each case, a 7-inch (180-mm)-diameter access hole was cut into the pipe 180 degrees from the defect area. For peening, a pneumatic scaler was put into the pipe and applied to the defect area. For quenching, the defect area was heated to red hot [1500°F (800°C)] by acetylene torch from the outside, and a water blast was used to cool the inner surface to  $\leq 500^\circ\text{F}$  (260°C) in 1 second or less. Figure 13 shows one of the test joints; Figure 14 shows an internal peened defect. In addition to the internal defects, several external surface defects were installed, such as the quench defect shown in Figure 15.

After the internal defects were installed, the coupons cut from the 7-inch access holes were tack-welded back into place. Later, on site at Rosen, the coupons were to be full-encirclement-welded to reduce the magnetic anomalies at the holes.

After the defects were installed and before the coupons were welded back into place, non-destructive measurements of surface stress patterns were made using a nonlinear harmonic (NLH) sensor. This technology is the preferred method for the laboratory since there was no magnet structure for deploying the Barkhausen probes on the inside curvature of the pipe. Figure 16 shows NLH measurements in progress.

Deployment of Barkhausen sensors in the pipe and on the outside required amplifier circuits to increase the signal level, filter out as much of the MFL signal energy as possible, and detect the radio-frequency signal, which could then be filtered to reduce the ripple noise. Six circuit boards were built. They could be used either in single-ended mode or differential. Figure 17 shows two of the boards.

In addition to the prefabricated defects, two additional defects were put into the test line in pipe segments provided by Rosen. The defects were made with a torch and water flood, as illustrated in Figure 18.



Figure 13. 16-inch test specimen after defects were installed



Figure 14. Internal peened defect



Figure 15. External quenched defect



Figure 16. Nondestructive surface stress measurements made to characterize internal and external defects prior to pull testing

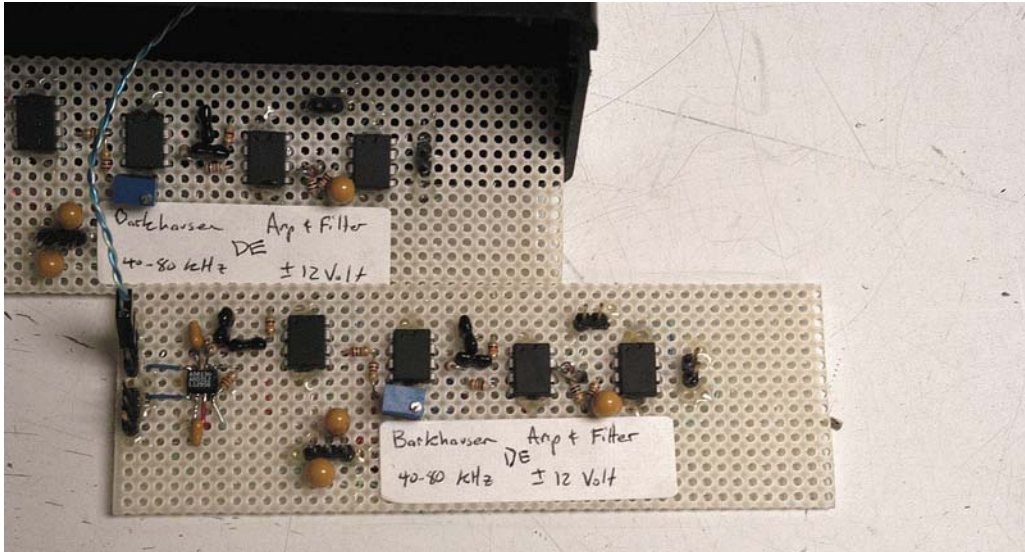


Figure 17. Amplifier/filter interface filter boards



Figure 18. Acetylene torch and water hose are used to make a quench zone on the test line

## 2.9 Rosen Pull Tests

On July 7–10, 2003, pull tests were run at the H. Rosen facility in Houston. The work was to test the feasibility of detecting local stress anomalies using a Barkhausen noise detector attached to the moving magnetizer of the Rosen MFL pig. Over the span of 4 days, 36 pull tests were run. Principal personnel were Al Crouch and Todd Goyen from SwRI and Thomas Beuker from Rosen Lingen. Stan Cone, Shawn Havard, and other Rosen technical personnel supported the work on the pull test line.

### 2.9.1 Test Line

The pull test line consisted of a 24.74-m assemblage of 5 pieces of 16-inch pipe. Figure 19 shows the pipe layout. Table 1 shows the details of the line.

Two test joints were prepared at SwRI and sent to Rosen to be installed into the line. In addition, Rosen added launch and receive trays and one transition joint before the first test joint.



Figure 19. Test line as seen from launch end

Table 1. Barkhausen Pull-Test Line

17-Jul-03

Pipe measurement reference is at 12:00 (0 degrees) at the start end of the pipe, with angle CW in direction of travel.

Pipe No. 1: Diameter = 16 inches, Wall Thickness = 0.375" (9.5 mm) Inlet tray.

| Axial Location<br>Distance from launch (m) | Angular Position<br>(Degrees) | Size | Item               |
|--|-------------------------------|------|--------------------|
| 0.00                                       | N/A                           |      | Start of Pipe      |
| 1.52                                       | 0                             |      | End of launch tray |
| 4.65                                       | N/A                           |      | Pipe girth weld    |

Pipe No. 2: Diameter = 16 inches, Wall Thickness = 0.188" (4.8 mm)

| Axial Location<br>Distance from launch (m) | Angular Position<br>(Degrees) | Size    | Item            |
|--|-------------------------------|---------|-----------------|
| 4.65                                       | N/A                           |         | Pipe girth weld |
| 6.49                                       | 0                             | 1" dia. | Grind marks     |
| 6.49                                       | 0, 270                        |         | OD sensors      |
| 7.70                                       | N/A                           |         | Pipe girth weld |

Pipe No. 3: Diameter = 16 inches, WT = 0.375 inches (9.5 mm) Grade X-52 Welded

| Axial Location<br>Distance from launch (m) | Angular Position<br>(Degrees) | Size             | Item                                    |
|--|-------------------------------|------------------|---|
| 7.70                                       | N/A                           |                  | Pipe girth weld                         |
| 8.17                                       | 90                            | 1" dia.          | Drilled Hole                            |
| 9.08                                       | 180                           | 7" dia.          | Hole with Coupon                        |
| 9.08                                       | 0                             | 2" ax. 10" circ. | Defect P1 - Peened Area on ID Surface   |
| 9.71                                       | 90                            | 3" dia.          | Defect P3 - Peened Area on OD Surface   |
| 10.30                                      | 180                           | 7" dia.          | Hole with Coupon                        |
| 10.30                                      | 0                             | 2" ax. 10" circ. | Defect Q1 - Quenched Area on ID Surface |
| 10.37                                      | 0, 270                        | N/A              | OD Sensors                              |
| 11.52                                      | 180                           | 7" dia.          | Hole with Coupon                        |
| 11.52                                      | 0                             | 2" ax. 10" circ. | Defect P2 - Peened Area on ID Surface   |
| 12.15                                      | 90                            | 3" dia.          | Defect Q3 - Quenched Area on OD Surface |
| 12.74                                      | 180                           | 7" dia.          | Hole with Coupon                        |
| 12.74                                      | 0                             | 2" ax. 10" circ. | Defect Q2 - Quenched Area on ID Surface |
| 13.66                                      | 90                            | 1" dia.          | Drilled Hole                            |
| 14.13                                      | N/A                           |                  | Pipe girth weld                         |

Pipe No. 4: Diameter = 16 inches, WT = 0.188 inches (4.8 mm) Grade X-52 Welded

| Axial Location<br>Distance from launch (m) | Angular Position<br>(Degrees) | Size             | Item                                    |
|--|-------------------------------|------------------|---|
| 14.13                                      | N/A                           |                  | Start of Pipe                           |
| 14.45                                      | 180                           | 1" dia.          | Drilled Hole                            |
| 15.36                                      | 180                           | 7" dia.          | Hole with Coupon                        |
| 15.36                                      | 0                             | 2" ax. 10" circ. | Defect P1 - Peened Area on ID Surface   |
| 15.96                                      | 90                            | 3" dia.          | Defect P3 - Peened Area on OD Surface   |
| 16.58                                      | 180                           | 7" dia.          | Hole with Coupon                        |
| 16.58                                      | 0                             | 2" ax. 10" circ. | Defect Q1 - Quenched Area on ID Surface |
| 17.80                                      | 180                           | 7" dia.          | Hole with Coupon                        |
| 17.80                                      | 0                             | 2" ax. 10" circ. | Defect P2 - Peened Area on ID Surface   |
| 18.41                                      | 90                            | 3" dia.          | Defect Q3 - Quenched Area on OD Surface |
| 19.01                                      | 180                           | 7" dia.          | Hole with Coupon                        |
| 19.01                                      | 0                             | 2" ax. 10" circ. | Defect Q2 - Quenched Area on ID Surface |
| 19.91                                      | 0                             | 2" ax. 10" circ. | ID Quench Defect - New                  |
| 19.93                                      | 180                           | 1" dia.          | Drilled Hole                            |
| 20.25                                      | N/A                           |                  | End of Pipe                             |

Pipe No. 5: Diameter = 16 inches, Wall Thickness = 0.375" (9.5 mm). Receiver tray

| Axial Location<br>Distance from launch (m) | Angular Position<br>(Degrees) | Size             | Item                   |
|--|-------------------------------|------------------|------------------------|
| 20.25                                      | N/A                           |                  | Pipe girth weld        |
| 21.19                                      | 0                             | 2" ax. 10" circ. | ID Quench defect - New |
| 22.53                                      | 0                             | 2" ax. 10" circ. | ID Quench defect - New |
| 23.22                                      | N/A                           |                  | Receive tray           |
| 24.74                                      | N/A                           |                  | End of Pipe            |

### 2.9.2 Defects

Each SwRI test joint had 11 artifacts installed, as described in Section 2.8.

### 2.9.3 Procedure

A farm tractor was used to pull the MFL pig section through the pipe. Speeds ranged from as slow as practical up to about 4 m/s. The MFL section had 360-degree coverage with flux leakage sensors. The Barkhausen sensors were attached to the magnetizer as shown in Figure 20, and electrical connections were brought out to the data acquisition instrument by a three-cable tag line. Amplification and filtering were provided at the pig site by circuitry inside a box mounted on the rear of the pig (Figure 21).

Data were acquired by a 12-bit A/D connected to a notebook computer. A digital oscilloscope with floppy disk storage was provided for high-speed sampling of the Barkhausen RF waveforms, and auxiliary instruments were on hand should we desire to do custom amplification/filtering of the signals. Figure 22 shows the instrumentation setup.



Figure 20. Sensor mounted rigidly to magnetizer. Note relief cut into urethane cup.

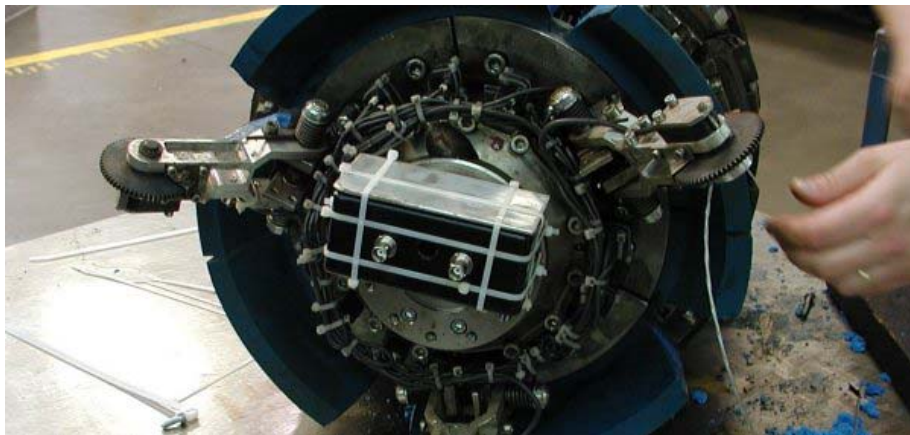


Figure 21. Amplifier box containing bandpass amplifiers and detector



Figure 22. Instrumentation complement for pull testing

### 2.9.4 Findings

Three sensor deployments were used on the MFL pig in these tests. The first tests were run with one sensor at the 10:30 position to compensate for pig roll during the pull test. This should have put the sensor at 12:00 at the middle of the run. Later tests were made with two sensors 120 degrees apart, fed to separate circuit cards and electronically differenced after playback. Launch was with one sensor at 12:00. The final arrangement was to take two sensors and stack them at one location on the pig. One was closer to the pipe surface by about 10 mm. The connection was again to two cards inside the circuit box. Pulls were run at speeds varying from 0.5 m/s to 3.5 m/s.

*Fixed Sensors*—In addition to the sensors on the pig, there were also sensors placed on the outside of the pipe. Two connected differentially were put on an OD quench spot in the heavy wall specimen. A grind mark was made on the top of the Rosen pup joint and a second differential pair attached there. In each OD case, one sensor was placed on the defect and the other at 90 degrees from it. Figures 23 and 24 show the external deployment for the quench spot and grind marks, respectively.

Analysis of the data from fixed sensors show little, if any, contribution from Barkhausen sources. The sensors are so overwhelmed by the strong magnetic field as the pig passes that the much smaller effects of Barkhausen transitions are swamped out. If it becomes necessary to retrieve Barkhausen signals from stationary sensors, an extremely sharp filter must be used to preserve the 40- to 80-kHz pass band of the Barkhausen noise and cut out the MFL signals that are many orders of magnitude larger.

Signals from the OD quench defect and the grind marks are shown in Figures 25 and 26. These waveforms are considered to be almost totally MFL in origin.



Figure 23. External sensors at external quench defect



Figure 24. External sensors at external grind mark

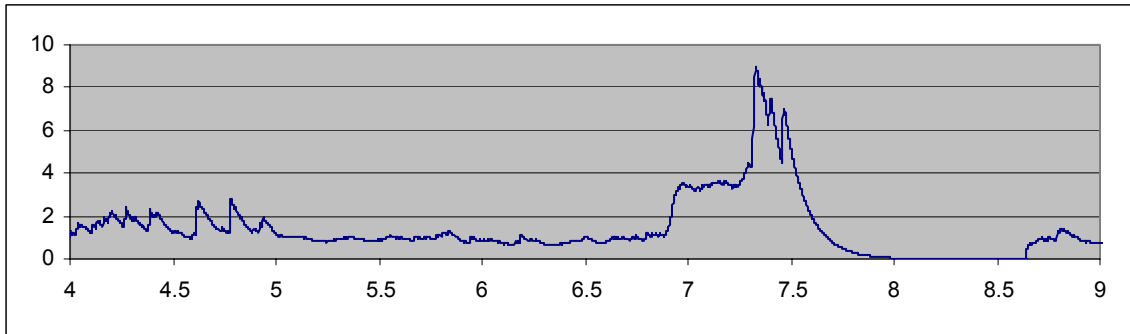


Figure 25. Differential signal from sensors at external quench defect

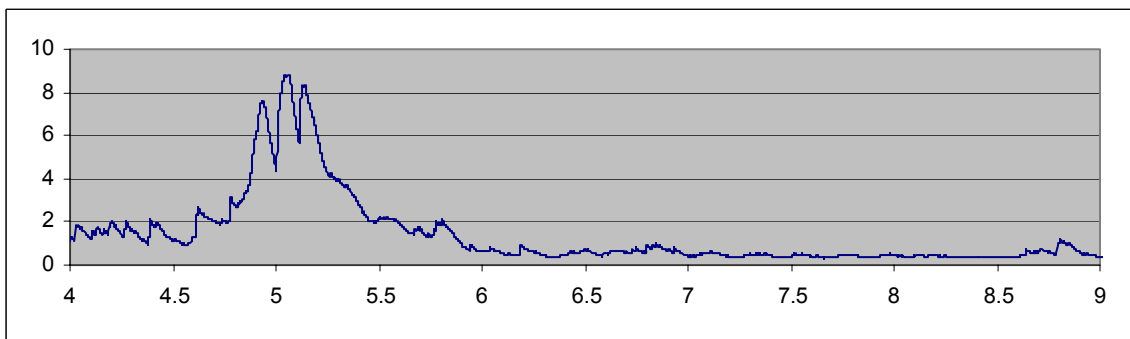


Figure 26. Differential signal from external grind marks

*Sensors on Pig*—The first few days were spent debugging the system and reducing noise. Samples of detected signals from the heavy wall and light wall pipe specimens are shown in Figures 27 and 28. For all runs, the separate sensors were recorded and the difference computed after the run.

The effects of noise can be reduced by differencing and filtering. For example, if a moving average filter is used on the arithmetic difference between the two sensors, one can reduce the waveforms to those combined in Figure 29. Here, the defects can be clearly seen. Repeatability was tested by comparing to another run with all parameters unchanged. That result is shown in Figure 30. Note the good repeatability.

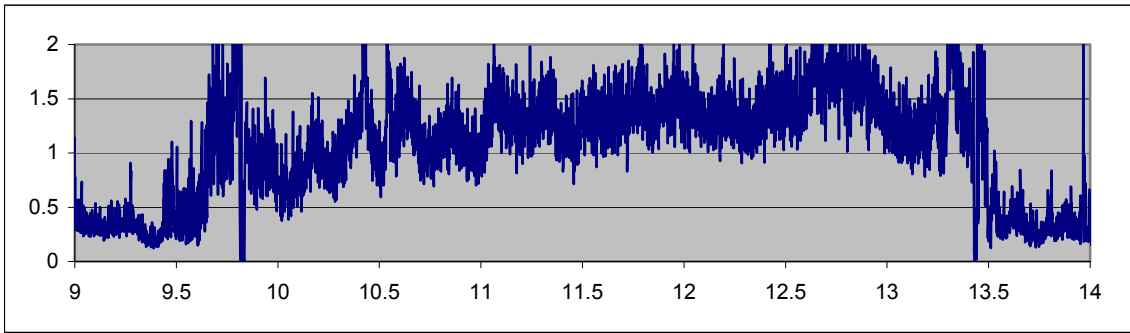


Figure 27. Heavy wall specimen

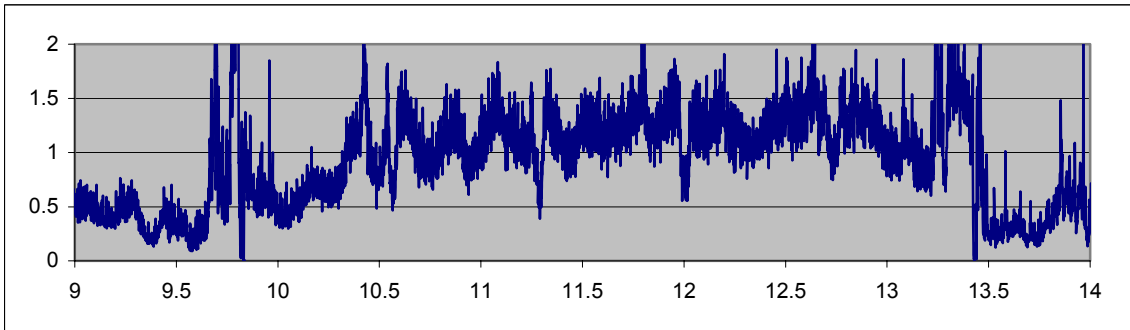


Figure 28. Light wall specimen

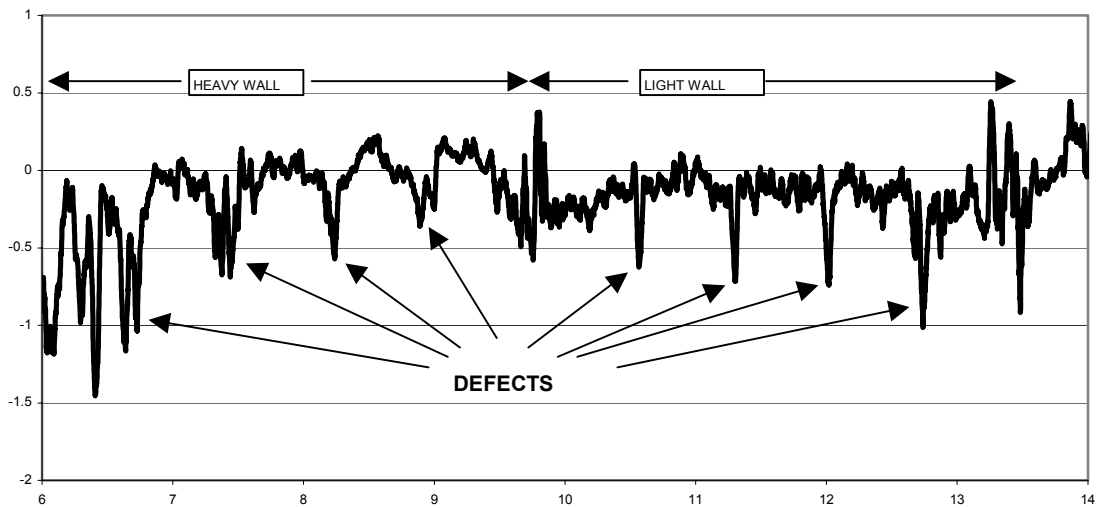


Figure 29. Differential sensor data smoothed with a running average filter

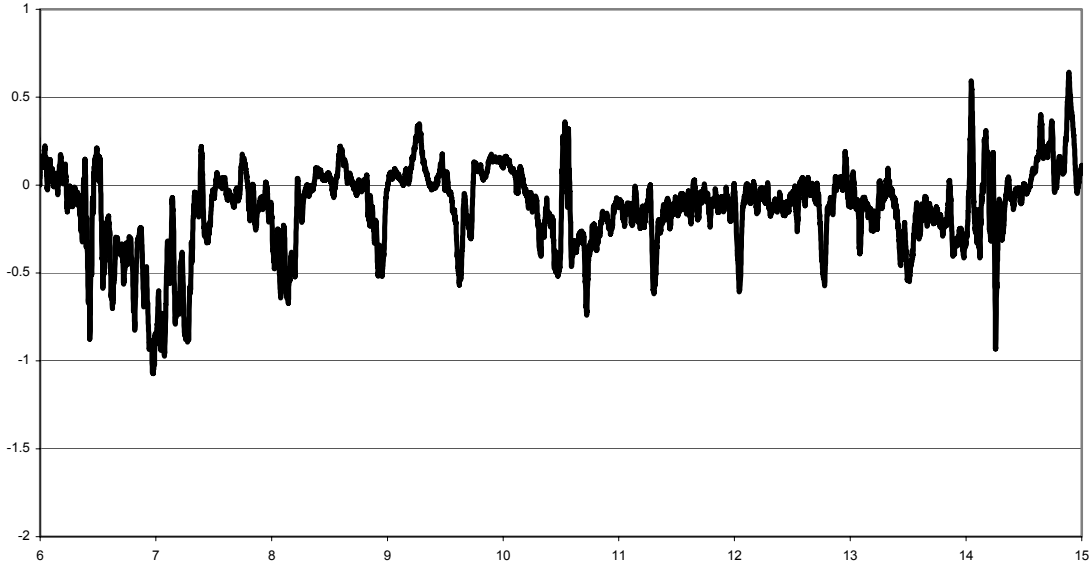


Figure 30. Smoothed differential data from subsequent run

### ***2.9.5 Conclusions from Rosen Pull Test***

The feasibility of detection of continuous Barkhausen by use of sensors on the magnetizer poles of an MFL pig was demonstrated. It was necessary to use difference probes to remove MFL noise sufficiently to make Barkhausen signals visible and to apply electronic filtering to increase the signal-to-noise ratio to an acceptable level.

Defects were detected over a range of pig speeds. The predominant speed effect was the Barkhausen signal amplitude, which increased with increasing pig speed.

## **3. CONCLUSIONS AND RECOMMENDATIONS**

### **3.1 CBN Measuring Ability**

As with any sensor system, the measuring performance of the continuous Barkhausen system will be affected by the linearity of the sensor's transfer function over the desired range of measurement and the signal to noise ratio achievable in the operating environment. Regrettably, we did not have calibrated defects to produce quantitative measures of the CBN measuring ability. The peened and quenched defects were anomalies in the pipe surface stress, but were not designed nor controlled to have a specific stress reading.

Significant filtering was employed to improve the signal-to-noise ratio. The frequency content of the raw Barkhausen data is fairly broad. We chose a 40kHz to 80 kHz pass band to avoid, as much as possible, the very strong induced MFL signals. The MFL influence was limited to approximately 1 kHz on the top end, so filter separation was easy to do. After detection of the RF envelope, low-pass filtering was used to clean the residual RF from the defect signal. We found that a cut-off frequency of about 6 Hz worked well.

### **3.2 Practical Considerations for Use on MFL Pig**

The electronics for using Barkhausen sensors on an MFL pig are relatively simple and can be fabricated in small packages consistent with the requirements of ILI hardware. Some adjustment of the low-pass filter cut-off frequency will be required to match the MFL pig speed.

The greatest challenge for applying the CBN sensors to the MFL pig will be the design of an adequate suspension system for the sensor coil(s). Attachment to trailing poles of the magnetizer has some advantages. First, the coil will be bumped away from the pipe wall when the magnetizer pole is bumped away. This will protect the coil from impact with girth weld drop-through or other protrusions into the pipe. Secondly, the coil moving with the pole piece helps minimize the induced MFL signals that are created by magnetizer pole movement.

## **4. FINANCIAL STATUS REPORT**

Total project funding of \$160,000 was provided equally by the Department of Transportation and our cofunding partner, H. Rosen Inspection.

DOT funds have been received. Rosen funding, consisting of \$50,000 cash and \$30,000 in-kind contribution, has also been received.

## 5. BIBLIOGRAPHY

The following articles are representative of Dr. David Atherton's work with Barkhausen technology at Queen's University in Kingston, Ontario. Further references may be found under Atherton's or Professor Lynann Clapham's names at the Queen's University web site. See, for example, [http://www.physics.queensu.ca/~amg/applied\\_magnetics.html](http://www.physics.queensu.ca/~amg/applied_magnetics.html).

- Birsan, M., J. A. Szpunar, T. W. Krause, and D. L. Atherton. "Correlation Between the Barkhausen Noise Power and the Total Power Losses in 3% Si-Fe," *J. Appl. Phys.* 79, (1996): 3156–3159.
- Birsan, M., J. A. Szpunar, T. W. Krause, and D. L. Atherton. "Magnetic Barkhausen Noise Study of Domain Wall Dynamics in Grain Oriented 3% Si-Fe," *IEEE Trans. on Magnetism* 32 (1996):527–534.
- Clapham, L., C. Jagadish, and D. L. Atherton. "The Influence of Pearlite on Barkhausen Noise Generation in Plain Carbon Steels," *Acta. Metall. Mater.* 39 (1991):1555–1562.
- Clapham, L., C. Jagadish, and D. L. Atherton. "The Influence of Controlled Rolling on the Pulse Height Distribution of Magnetic Barkhausen Noise in Steel," *Materials Science and Engineering A145* (1991):233–241.
- Dhar, A., and D. L. Atherton. "Correlation Between Magnetic Flux Leakage and Magnetic Barkhausen Noise in Steel Pipelines," *British J. Nondestructive Testing* 35 (1993):307–309.
- Dhar, A., and D. L. Atherton. "Effects of Magnetic Flux Density and Tensile Stress on the Magnetic Barkhausen Noise in Pipeline Steel," *Nondestructive Testing and Evaluation* 10 (1993):287–294.
- Dhar, A., and D. L. Atherton. "Flux Density Dependence of Magneto-Acoustic Emission in Pipeline Steel," *J. Appl. Phys.* 72 (1992):601–606.
- Dhar, A., and D. L. Atherton. "The Influence of Magnetizing Parameters on the Magnetic Barkhausen Noise," *IEEE Trans. on Magnetism* 28 (1992):3363–3366.
- Dhar, A., and D. L. Atherton. "Magnetizing Frequency Dependence of Magneto-Acoustic Emission in Pipeline Steel," *IEEE Trans. on Magnetism* 28 (1992):1003–1007.
- Dhar, A., L. Clapham, and D. L. Atherton. "Effect of Sweep and Bias Field Amplitudes on the Magneto-Acoustic Emission," *IEEE Trans. on Magnetism* 27 (1991):5364–5366.
- Dhar, A., C. Jagadish, and D. L. Atherton. "The Effect of Sample Size on Magneto-Acoustic Emission," *NDT International* 24 (1991):15–19.
- Dhar, A., C. Jagadish, and D. L. Atherton. "Using the Barkhausen Effect to Determine the Easy Axis of Magnetization in Steels," *Materials Evaluation* 50 (1992):1139–1141.

- Gauthier, J. "Magnetic Barkhausen Noise and Acoustoelasticity: A Comparison of Two Non-Destructive Methods of Measuring Residual Strain." M.Sc. dissertation, Queen's University, 1994.
- Jagadish, C., L. Clapham, and D. L. Atherton. "Effect of Bias Field and Stress on Barkhausen Noise in Pipeline Steels," *NDT International* 22 (1989):297–301.
- Jagadish, C., L. Clapham, and D.L. Atherton. "The Effect of Stress and Magnetic Field Orientation on Surface Magnetic Barkhausen Noise in Pipeline Steel," *IEEE Trans. on Magnetics* 26 (1990):262–265.
- Jagadish, C., L. Clapham, and D. L. Atherton. "The Influence of Stress on Surface Barkhausen Noise Generation in Pipeline Steels," *IEEE Trans. on Magnetics* 25 (1989):3452–3454.
- Jagadish, C., L. Clapham, and D. L. Atherton. "Influence of Sweep Rate on the Power Spectrum and Pulse Height Distribution of Barkhausen Noise in Pipeline Steel," *Nondestr. Test Eval.* 5 (1990):271–275.
- Jagadish, C., L. Clapham, and D. L. Atherton. "Influence of Uniaxial Elastic Stress on Power Spectrum and Pulse Height Distribution of Surface Barkhausen Noise," *IEEE Trans. on Magnetics* 26 (1990):1160–1163.
- Jagadish, C., L. Clapham, and D. L. Atherton. "Orientation Effects of Anisotropy, Stress, Excitation, Bias, and Residual Fields on Barkhausen Noise Generation in Pipeline Steel," *J. Phys. D: Appl. Phys.* 23 (1990):443-448.
- Jagadish, C., L. Clapham, and D. L. Atherton. "Surface Barkhausen Noise Measurements of Stress and Leakage Flux Signals in Line Pipe," *Review of Progress in Quantitative Nondestructive Evaluation*, Vol. 9A, pp. 1871–1878. Edited by D. O. Thompson and D. E. Chimenti. New York: Plenum, New York, 1990.
- Krause, T. W., and D. L. Atherton. "High Resolution Magnetic Barkhausen Noise Measurements," *NDT&E Int.* 27 (1994):210–207.
- Krause, T. W., and D. L. Atherton. "High Resolution Magnetic Barkhausen Noise Measurements of Slit Defects in Steel," presented at *ASNT Fall Conference*, Nov. 8–12, 1993, Long Beach, California.
- Krause, T. W., D. L. Atherton, and S. P. Sullivan. "Magnetic Barkhausen Noise Indicators of Cracks in Steel," *Nondestructive Test and Evaluation* 13 (1997):309–323.
- Krause, T. W., L. Clapham, and D. L. Atherton. "Characterization of the Magnetic Easy Axis in Pipeline Steel Using Magnetic Barkhausen Noise," *J. Appl. Phys.* 75 (1994)7983–7988.
- Krause, T. W., L. Clapham, A. Pattantyus, and D. L. Atherton. "Investigation of the Stress-Dependent Easy Axis in Steel Using Magnetic Barkhausen Noise," *J. Appl. Phys.* 79 (1996):4242–4252.

- Krause, T. W., J. M. Makar, and D. L. Atherton. "Investigation of the Magnetic Field and Stress Dependence of 180° Domain Wall Motion in Pipeline Steel Using Magnetic Barkhausen Noise," *J. Magnetism and Magnetic Materials* 137 (1994):25–34.
- Krause, T. W., A. Pattantyus, and D. L. Atherton. "Investigation of Strain Dependent Magnetic Barkhausen Noise in Steel," *IEEE Trans. on Magnetics* 31 (1995):3376–3378.
- Krause, T. W., N. Pulfer, P. Weyman, and D. L. Atherton. "Magnetic Barkhausen Noise: Stress-Dependent Mechanisms in Steel," *IEEE Trans on Magnetics* 32 (1996):4764–4766.
- Krause, T. W., J. A. Szpunar, M. Birsan, and D. L. Atherton. "Correlation of Magnetic Barkhausen Noise with Core Loss in Si-Fe Steel Laminates," *J. Appl. Phys.* 79 (1996):3156–3167.
- Mandal, K., D. Dufour, R. Sabet-Shargi, B. Sigers, D. Micke, T. W. Krause, L. Clapham, and D. L. Atherton. "Detection of Stress Concentrations Around a Defect by Magnetic Barkhausen Noise Measurements," *J. Appl. Phys.* 80 (1996):6391–6395.
- Mandal, K., M. E. Luoukas, A. Corey, and D. L. Atherton. "Magnetic Barkhausen Noise Indications of Stress Concentrations Near Pits of Various Depths," *J. Magnetism and Magnetic Materials* 175, (1997):255–262.

**Appendix A**  
**GUIDELINES FOR COMMERCIAL DEVELOPMENT**

# Appendix A

## GUIDELINES FOR COMMERCIAL DEVELOPMENT

This report substantiates the claim that basic feasibility has been shown for using a moving magnetic flux leakage (MFL) magnetizer to generate Barkhausen noise that can be detected by a suitable sensor attached to the magnetizer. Enough of the operating characteristics of the Continuous Barkhausen (CBN) system were learned to allow us to offer guidelines for continuation of the project into a commercialization phase. The following discussion covers the topics to be considered by the system designer when designing a CBN commercial system.

### SENSOR DESIGN

The Barkhausen sensor, as described in the report, is a wire coil placed near the pipe surface in a region of high magnetic gradient. To be consistent with the prototype system, the commercial sensor will have the following characteristics

1. *Coil size*—A rectangular loop with a long side (length) transverse to the pipe and pig axes. The loop will be short in the direction of travel (width) and will have a nonmetallic core with a height on the order of the width. Typical dimensions, which offer a good starting point are: length = 20 mm, width 6 mm, height 6 mm. It is preferable that the coil be layer-wound with magnet wire. Wire size from AWG 30 to AWG 40 should be acceptable. The smaller wire sizes will produce a better signal-to-noise ratio (SNR) due to their greater number of turns, but will require extra care to avoid breakage during winding. The prototype coil contained 500 turns of wire.
2. *Connection*—A single-ended (absolute) system should produce usable defect signals, but superior performance will be afforded by the addition of second coil in a differential connection. Differential pairs significantly reduce the noise from pig movement and external electrical sources such as lightning. In developing the prototype system, it was learned that a differential pair, with one coil very near the pipe surface and the other immediately above the first, functioned well.
3. *Liftoff*—A simple guideline is that the primary coil (the one closest the pipe) should be as close to the pipe as possible without risking damage to the coil from contact with the pipe surface. Fortunately, the Barkhausen signal does not fall off extremely rapidly with liftoff, permitting the designer to start with a reasonable gap—for example, 1 mm. Further, attachment of the coil to a magnetizer pole (see No. 4 below) helps protect the coil from impacting welds or other pipeline artifacts.
4. *Location*—Analytical modeling showed the optimum position for the CBN sensor to be between the pole face and the pipe near the trailing edge of the pole. It is conceivable that recesses could be provided in the pole face and sensors placed there, with protection from external forces provided by epoxy or other nonmetallic material between the coil and the pipe surface. Alternatively, the coil could be attached to the trailing face of the pole, as was done

in the field experiment described in this report. Embedded sensors would be much more rugged and would be well-protected from impacts with hanging weld flash and other edges in the pipe.

5. *Number*—The number of sensor channels and their spacing around the pipe circumference is affected by the size of defects being sought. If the CBN system has mechanical damage as its target defect, the typical defect will be on the order of 100 mm or more in extent. This means that sensors no more than 50 mm apart should not miss any defect. Better characterization of the defect will be achieved if the spacing is closer—for example, 25 mm. As a practical matter, one should tailor the sensor deployment to the size of the MFL pole pieces. If a pole piece is 100 mm in circumferential extent, perhaps four sensors could be fit into each pole piece. The pipe size will then determine the required number of sensors. For example, 24-inch pipe may require 64 to 80 sensors.
6. *Sensor Suspension*—If the sensor is embedded into the magnetizer pole face, no separate suspension is needed. If the sensor is attached closely to the trailing edge of the pole face, again, no additional suspension components should be required. However, if there is a compelling reason to maintain a gap between the CBN sensor and the magnetizer pole, it may be necessary to provide separate holders for the sensors. The holders should have sufficient radial compliance so that the sensors can tolerate impact from girth weld flash and other protrusions into the pipe. They should be able to hold the sensors close to the pipe surface and keep them in proper angular alignment.

## ELECTRONICS

The electronics required to interface between the CBN sensors and the data acquisition and storage functions of the smart pig are relatively simple. The three required functions are amplification, filtering, and detection.

1. *Amplification*—Signals from the sensor coil depend on magnetic field strength, number of turns of the sensor coil, and pig speed. Typical signal levels encountered in the pull test were on the order of 100  $\mu$ V. Therefore, one would provide gain of approximately 10-20,000. Gain adjustment of at least 20 dB is recommended.
2. *Filtering*—Experimental data showed that an acceptable SNR could be obtained by using a 40- to 80-kHz bandpass filter on the RF data. The 40-kHz low-end cutoff is sufficiently high to effectively remove all the magnetic flux leakage signals that may be induced into the coil. The 80-kHz upper end is as low as it can be without removing noticeable amounts of the Barkhausen signal. Besides the RF filtering, there is also low-pass filtering of the detected signal. That frequency will depend on pig speed and size of the inspection target. A filter frequency on the order of 20 Hz is recommended.
3. *Detection*—In all the experimental work, detection of the RF signal was achieved with a simple diode detector and integrating capacitor. It is recommended that a germanium diode be used to reduce the voltage drop inherent in rectification. The detected signal should be filtered as discussed above.

Amplification and filtering are functions found in all MFL systems, so if CBN capability is to be added to an existing MFL system, one should first consider the existing electronic designs to determine if there is commonality enough to take advantage of the existing designs.

## CALIBRATION

The pull testing done for this report used only simulated defects—peened and quenched areas on the inside pipe surface. They were all detected with acceptable SNR, but there was no quantitative comparison done to the severity of the defect. The preferred way to gather the data to make that calibration is by use of a four-point bending specimen in a pull-test line. Four-point bending creates regions of uniform bend stress between the inner support members, compressive on one side of the bend and tensile on the other, with a neutral plane between. So, if one had a full complement of CBN sensors on a pig and pulled it through such a bend fixture, one should observe the full range of responses from maximum positive signal (tensile stress) through zero to maximum negative signal (compressive stress). These pull runs should produce data that could be compared to field measurements to gauge the severity of defects detected in the field.

## DATA ANALYSIS

The simple approach for data analysis used to date has been signal amplitude only, using the filtered detected signal. If more advanced data treatment is needed or desired for enhancement, there are several other approaches that have been used with conventional Barkhausen NDE.

1. *Frequency discrimination*—Barkhausen noise is wideband, with content from low frequencies up through several megahertz. As mentioned above, we used the 40- to 80-kHz band. As an alternative, one could separate the Barkhausen energy into discrete frequency bands and compare outputs at two or more bands, or produce a distribution curve showing amplitude versus frequency and compare curves on good pipe versus defective areas.
2. *Amplitude discrimination*—The Barkhausen noise consists of bursts of various amplitude pulses. There may be information in the distribution of pulse amplitudes. That information could be retrieved by either separating signal content in various amplitude level windows, or by computing an amplitude distribution curve for the output over some time window.
3. *Geometric analysis*—Pipeline bends create residual stress pairs, diametrically opposed in the pipe. Differential analysis of outputs of sensors separated by 180 degrees could reveal whether the CBN was the result of a pipe bend and would identify the plane of the bend. Further, geometric data could help identify the type of defect. A dent-like signal on the bottom of the pipe would likely be a rock dent, whereas a similar defect indication on the top of the pipe might be the result of third-party contact.